THE UNIVERSITY of EDINBURGH

Edinburgh Research Explorer

Coherent control in the continuum: autoionization of Xe

Citation for published version:
Fielding, HH & Kirrander, A 2007, 'Coherent control in the continuum: autoionization of Xe', *Journal of Physics B: Atomic, Molecular and Optical Physics*, vol. 40, no. 5, 897. https://doi.org/10.1088/0953-4075/40/5/006

Digital Object Identifier (DOI):
10.1088/0953-4075/40/5/006

Link:
Link to publication record in Edinburgh Research Explorer

Document Version:
Publisher's PDF, also known as Version of record

Published In:
Journal of Physics B: Atomic, Molecular and Optical Physics

General rights
Copyright for the publications made accessible via the Edinburgh Research Explorer is retained by the author(s) and / or other copyright owners and it is a condition of accessing these publications that users recognise and abide by the legal requirements associated with these rights.

Take down policy
The University of Edinburgh has made every reasonable effort to ensure that Edinburgh Research Explorer content complies with UK legislation. If you believe that the public display of this file breaches copyright please contact openaccess@ed.ac.uk providing details, and we will remove access to the work immediately and investigate your claim.

Download date: 05. May. 2023

IOP Publishing Journal of Physics B: Atomic, Molecular and Optical Physics

J. Phys. B: At. Mol. Opt. Phys. **40** (2007) 897–908 doi:10.1088/0953-4075/40/5/006

Coherent control in the continuum: autoionization of Xe

A Kirrander and H H Fielding

Department of Chemistry, University College London, 20 Gordon Street, London WC1H 0AJ, UK

E-mail: h.h.fielding@ucl.ac.uk

Received 19 December 2006, in final form 10 January 2007
Published 12 February 2007
Online at stacks.iop.org/JPhysB/40/897

Abstract

We explore, by time-dependent MQDT calculations, the potential for coherent control of autoionization using phase-shaped optical pulses. We investigate the effect of step-like spectral phase modulation on the autoionization dynamics of Rydberg wave packets in the Xe atom. It is found that a single step in the spectral phase has a substantial effect on the branching ratio, if the position of the step corresponds to a resonance in the Rydberg system. These effects are enhanced if the optical pulse is engineered to have multiple steps that reflect the periodicity inherent in Rydberg systems. Further calculations indicate that, to a large extent, the effects of phase manipulations are additive and independent. We also compare this new approach with approaches based on sequences of identical coherent optical pulses. The two methods are complementary, and we suggest that in the future they may be combined.

1. Introduction

During the last 15 years increasingly rapid progress has been made in the area of coherent control [1, 2]. The ability to control the dynamics of quantum mechanical systems is a fascinating development in modern physics, and includes selective population transfer in atoms and molecules, and the steering of the dynamics of bound and free electrons (see e.g. [3] and references in [4]).

Of great importance in this field is the development of techniques for the generation of shaped femtosecond optical pulses [5]. Ultrashort optical pulses can be shaped into target wave forms by intensity and phase modulation of the original spectrally dispersed pulse. In principle, such spectral phase and amplitude filtering techniques can produce almost any arbitrary pulse shape. Recently Renard *et al* [6] demonstrated that substantial control over the pulse shape can be achieved by shaping of the phase only.

In this paper we explore the potential of such phase-shaped pulses for coherent control of autoionizing states of Xe, and compare this with the results achieved using trains of identical

 © 2007 IOP Publishing Ltd Printed in the UK

coherent pulses. In particular, we are interested in the opportunities to control the branching ratio between the separate ionization channels. Controlling the branching ratio for nonradiative decay of excited states in atoms and molecules is a problem of continuing interest in physics.

2. Theory

2.1. Time-dependent MQDT

Time-dependent methods to calculate quantum dynamics broadly fall in two groups. The first category of methods propagates a wave packet, thereby exploring relevant regions of available phase space [7, 8]. The second category of methods follows the dynamics of the system by forming a coherent superposition of stationary states of different energy. This is particularly useful for Rydberg systems, where multichannel quantum defect theory (MQDT) provides exceptionally accurate energies and wavefunctions for the system. A number of workers have used this to explore wave packet dynamics in Rydberg systems, both in the discrete [9, 10] and the autoionizing [11–14] regions of the spectrum. In the following we use the approach of Fielding *et al* [12] for autoionizing Rydberg states.

The time-dependent autoionization cross-sections are proportional to

$$\sigma_i(t) \propto \left| \int \mathrm{d}E\, \mathrm{e}^{-\imath Et} G(E)\, \mathrm{d}_i^{(-)}(E)\sqrt{E} \right|^2 \tag{1}$$

in the limit of impulsive weak-field excitation. The spectral profiles $G(\omega)$, equivalent to $G(E)$ in atomic units, are investigated further in section 3. The total cross section is the incoherent sum of the partial cross sections,

$$\sigma(t) = \sum_{i\,\in\,\mathrm{open}} \sigma_i(t) \tag{2}$$

and the branching ratio for each channel, B_i, is obtained as

$$B_i = \frac{\int \mathrm{d}t\, \sigma_i(t)}{\int \mathrm{d}t\, \sigma(t)}. \tag{3}$$

The resonant dipole transition moments $d_i^{(-)}$ in equation (1) are obtained by MQDT. We review briefly the MQDT equations for autoionizing states in the following, but for an in-depth discussion we refer the reader to one of the excellent reviews that exist on the topic [15, 16]. In essence, MQDT is a subset of scattering theory. It exploits the fact that complicated many-electron interactions in a Rydberg atom or molecule are localized to an inner reaction volume, outside of which a single-electron view is essentially correct.

The boundary conditions on the MQDT wavefunction are such that the wavefunction must vanish exponentially in closed channels when $r \to \infty$, while in open channels it must have a phase shift $\pi\tau$. This can be written in the form of the generalized eigenvalue equation

$$\Gamma_{i\alpha}(E) A_{\alpha\rho}(E) = \tan \pi\tau_\rho(E) \Lambda_{i\alpha} A_{\alpha\rho}(E), \tag{4}$$

where

$$\Gamma_{i\alpha}(E) = \begin{cases} U_{i\alpha} \sin \pi(\nu_i + \mu_\alpha), & i \in \text{closed} \\ U_{i\alpha} \sin \pi\mu_\alpha, & i \in \text{open} \end{cases} \tag{5}$$

and

$$\Lambda_{i\alpha}(E) = \begin{cases} 0, & i \in \text{closed} \\ U_{i\alpha} \cos \pi\mu_\alpha, & i \in \text{open} \end{cases} \tag{6}$$

for closed and open channels i respectively. The accumulated phase in closed channels is $\beta_i = \pi(\nu_i - l_i)$, where l_i is the orbital angular momentum of the electron and $\nu_i = \sqrt{-R/(E - E_i^+)}$ is the effective principal quantum number, where R is the Rydberg constant and E_i^+ is the ionization limit. The number of non-trivial solutions to equation (4) equals the number of open channels. Each ρth solution vector must be normalized

$$\sum_{i\in\text{open}} \left(\sum_{\alpha} U_{i\alpha} \cos \pi[\mu_\alpha - \tau_\rho(E)] A_{\alpha\rho}(E) \right)^2 = 1. \tag{7}$$

Having thus obtained the collision eigenchannel solutions $A_{\alpha\rho}(E)$, and the collision eigenchannel phase shifts $\pi\tau_\rho(E)$, it is now straightforward to calculate the dipole transition moments to each collision eigenchannel,

$$d_\rho(E) = \sum_\alpha d_\alpha(E) A_{\alpha\rho}(E), \tag{8}$$

where $d_\alpha(E)$ are the transition moments in the close-coupled channels. In order to obtain the probability of ejection of a photoelectron into any specific ionization channel, we then construct a travelling wavefunction as a superposition of collisional eigenchannel functions that satisfy the incoming wave boundary condition at infinity so that the amplitude of the outgoing wave vanishes in all open channels $i \neq j$. This gives

$$d_i^{(-)}(E) = \sum_\rho \mathrm{e}^{\imath\eta_i(E)} T_{i\rho}(E)\, \mathrm{e}^{\imath\pi\tau_\rho(E)} d_\rho(E), \tag{9}$$

where $T_{i\rho}$ is an orthonormal $N_o \times N_o$ matrix with elements

$$T_{i\rho}(E) = \sum_\alpha U_{i\alpha} \cos(\pi\mu_\alpha - \pi\tau_\rho) A_{\alpha\rho} \tag{10}$$

and, in a Coulomb potential,

$$\eta_i(E) = (1/k_i) \ln 2k_i - l_i\pi/2 + \arg\Gamma(l_i + 1 - \imath/k_i), \tag{11}$$

where $k_i = \sqrt{2(E - E_i^+)}$ is the linear momentum of an electron in open channel i.

2.2. Xe

The Xe atom has long been an important model system for theoretical studies of autoionizing spectra [17, 18], and has frequently been re-visited in novel and interesting experiments [19–21]. The present paper concerns the Rydberg states of Xe between the first and second ionization limit with total angular momentum $J = 1$ (excluding nuclear spin), accessed by a single photon from the ground state. This part of the spectrum contains five dipole-allowed Rydberg channels. Each channel is identified by the state of the core and the Rydberg electron. A good description of the angular momentum is jl coupling; the Xe^+ ion core is LS-coupled with $L^+ + S^+ = J^+$, and the total angular momentum of the core J^+ couples to the orbital angular momentum l_i of the Rydberg electron, $J^+ + l_i = K_i$, and finally the angular momentum K_i couples to the spin of the Rydberg electron, $K_i + s_i = J$.

The first and second ionization limits correspond to the ground $^2P_{3/2}$ and the first excited $^2P_{1/2}$ states of Xe^+, respectively. In this region the atom has two closed channels, which autoionize by coupling to three continuum channels. The two bound series converge to the second ionization limit and correspond to excitation of an outer $p_{1/2}$ electron to $ns_{1/2}$ (sharp resonances) or $nd_{3/2}$ (diffuse resonances) channels, while the three continuum channels correspond to the excitation of an outer $p_{3/2}$ electron to $\epsilon s_{1/2}$, $\epsilon d_{3/2}$ or $\epsilon d_{5/2}$ continuum states [18], where ϵ is the energy above the lower ionization limit.

We use the quantum defects, the transformation matrix and the transition moments from the relativistic MQDT calculations by Johnson *et al* [18]. These calculations take the spin–orbit coupling into account. Atomic data for Xe are obtained from NIST [22].

3. Optical pulses

3.1. Sequence of coherent pulses

Sequences of identical coherent pulses have been used successfully for control in many Rydberg experiments in both atoms and molecules [20, 21]. We take this opportunity to revisit the theory and to present both frequency and time-domain interpretations of control schemes based on two identical pulses. The effect of a two-pulse control scheme on the autoionization of Xe is investigated.

Quite generally, a train of N identical pulses $G(t)$ centred at times t_k,

$$f_N(t) = \sum_k^N G(t - t_k) \tag{12}$$

has the Fourier transform

$$F_N(\omega) = G(\omega) \sum_k^N \mathrm{e}^{\imath\omega t_k}. \tag{13}$$

This follows from the linearity and time-shifting properties of Fourier transforms [23, 24]. In the limit of many identical pulses, equation (13) describes a sharp optical frequency comb [25]. The actual pulse shape determines the spatial localization of the excited wave packet [26], but does not influence the emergence of a comb-like structure in the optical power spectrum.

For a pulse train, with one pulse at time t_1 and a second pulse at time $t_1 + \delta_t$, we can write the Fourier transform $F_2(\omega)$ as

$$F_2(\omega) = G(\omega)\cos(\omega\delta_t/2)\exp[\imath\omega(t_1 + \delta_t/2)]. \tag{14}$$

In particular, note that the envelope in equation (14) is modulated by a cosine term. The resulting comb has an optical power spectrum proportional to $|\cos(\omega\delta_t/2)|$, with peaks spaced by

$$\Delta\omega = 2\pi/\delta_t. \tag{15}$$

The position of the peaks can be shifted by an angle θ in the cosine term. This can be achieved by an additional time delay $2\theta/\omega_0$, since $\omega(\delta_t + 2\theta/\omega_0)/2 \approx \omega\delta_t/2 + \theta$, where ω_0 is the central frequency of the laser pulse. A shift of $\theta = \pi/2$, for instance, swaps the positions of the peaks and the troughs in the comb. Finally, the comb can be centred at the central laser frequency ω_0 by adding an additional time delay $\gamma = -(1/\omega_0)\mathrm{mod}(\omega\delta_t, 2\pi)$.

From the Rydberg formula, $E_n \propto (n - \mu)^{-2}$, it follows that for large principal quantum numbers n the energy spacing is $\Delta E = n^{-3}$, and that the quantum defect μ shifts the energy by μn^{-3} to first order. A wave packet excited at a central frequency ω_0 has principal quantum number $\overline{n}$ and a classical Kepler orbit period of $T_{cl} = 2\pi/\Delta E = 2\pi\overline{n}^3$. Substituting the expression for T_{cl} into equation (15) it follows that $\delta_t = T_{cl}$ gives a $1/\overline{n}^3$ spacing in the comb, i.e. the resulting comb overlaps with all states in a Rydberg series. A delay $\delta_t = T_{cl}/2$, on the other hand, gives a spacing of $0.5/\overline{n}^3$, and so only every second state is excited. This means that it is possible to select either even n or odd n states. The Schrödinger's cat states of Noel and Stroud [27] can be interpreted in this framework.

An even more interesting scenario occurs when there are two Rydberg series with the same ionization limit present. The spacing between the levels in the two series is approximately

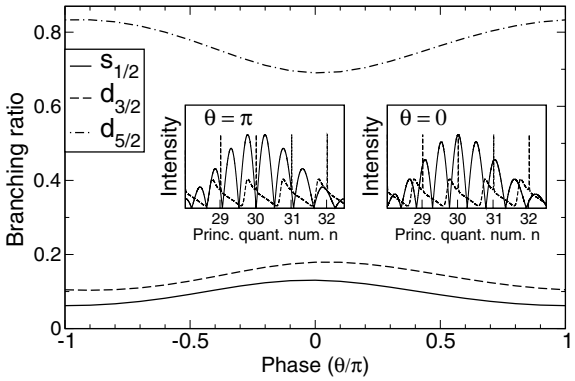

Figure 1. Branching ratio for ionized electrons in the three open channels as a function of $\theta \in [-\pi, \pi]$ for a time delay $\delta_t = 2T_{cl} + \theta/\omega_0$ between two coherent 1 ps Gaussian pulses centred at $\overline{n} = 30.0188$. The insets show the optical power spectrum for $\theta = \pm\pi$ and $\theta = 0$ respectively, with the total photoionization cross-section plotted in the background for guidance.

$\Delta\mu/\overline{n}^3$, where $\Delta\mu = \mu_2 - \mu_1$, and where μ_1 and μ_2 are quantum defects characteristic of each Rydberg series. Maximum selectivity between the two series is achieved when the peaks of the comb coincide with one series and the troughs with the other, which occurs when the time delay $\delta_t = T_{cl}/2\Delta\mu$ and the spacing of the comb is $2\Delta\mu/\overline{n}^3$. For instance, when $\Delta\mu = 0.25$, the required delay time is $\delta_t = 2T_{cl}$. A small additional time delay will shift the comb for maximum overlap with one series and minimum overlap with the other. The difference in quantum defect between the two autoionizing series ns and nd in Xe is $\Delta\mu \approx 0.25$, so the example above is highly relevant to the present work.

We now discuss the same control scheme from a time-domain perspective. Here the time evolution of the excited Rydberg wave packet becomes of central importance. The phase evolution of a wave packet excited around the central excitation frequency ω_0 can be examined by a Taylor expansion [28, 29]

$$\exp(\imath\omega_0 t) \approx \exp\left(-\frac{\imath}{2\overline{n}^2}\left[1 - 2\frac{\delta\nu}{\overline{n}} + 3\left(\frac{\delta\nu}{\overline{n}}\right)^2 - \cdots\right]t\right), \tag{16}$$

with $\nu = n - \mu$ and $\delta\nu = \overline{n} - \nu$. From equation (16) it is clear that the phase evolution has a component due to the quantum defect μ. Hence, the phase difference Φ between two channels is proportional to the difference in quantum defects $\Delta\mu$,

$$\Phi(t) = \frac{2\pi\Delta\mu}{T_{cl}}t. \tag{17}$$

Equation (17) is key to the time-domain interpretation of the two pulse coherent control scheme. It has a semiclassical interpretation where the oscillating Rydberg wave packet acquires a phase kick proportional to the quantum defect during each collision with the ion core, and where t/T_{cl} counts the number of collisions. In our case, where $\Delta\mu = 0.25$, the two components of the wave packet will be approximately $\Phi = \pi$ out of phase at time $t = 2T_{cl}$. A second pulse at that time will interfere destructively with one component and constructively with the other.

Both the frequency and time domain analysis shows that a time delay of $\delta_t = 2T_{cl} + \theta/\omega_0$ will be most efficient in selecting between the $n\mathrm{s}_{1/2}$ and $n\mathrm{d}_{3/2}$ autoionizing series in Xe. We calculated the ionization branching ratio with the parameter $\theta \in [-\pi, \pi]$ using two identical 1 ps FWHM Gaussian pulses centred at principal quantum number $\overline{n} = 30.0188$. Figure 1

shows the branching ratio for the three open channels as a function of θ. The branching ratios have maxima and minima at $\theta = \pm\pi$ and $\theta = 0$, respectively. The $\epsilon s_{1/2}$ channel has a maximum at $\theta = 0$ and a minimum at $\theta = \pm\pi$. The insets in figure 1 show that these points correspond to maximum respectively minimum overlap of the optical spectrum with the $ns_{1/2}$ resonances.

It is worth noting that figure 1 shows that we cannot achieve completely independent control over the ionization into each open channel in the present two pulse scheme. The reason, essentially, is that the two pulse scheme relies on the different decay characteristics of the closed channels. Since, in this case, the number of open channels is greater than the number of closed channels, there will always be some degree of correlation between the branching ratios into the different open channels [30, 31]. Also, close inspection of figure 1 reveals that while the branching ratio for the $\epsilon s_{1/2}$ channel is symmetric around $\theta = 0$, the two d-electron channels are somewhat asymmetric. This can be understood in terms of the different q-parameters for the $ns_{1/2}$ and $nd_{3/2}$ resonances. The $ns_{1/2}$ resonances are almost symmetric at the resolution of the pulse, while the broad $nd_{3/2}$ resonances have a marked asymmetry [32, 33].

The degree of control can be fine tuned by adding a chirp to one of the two pulses [29]. In the time domain this corresponds to a second-order term in the phase evolution of the wave packet that compensates for the dispersion of the wave packet. A complementary view is that the chirp improves the overlap in the wings of the power spectrum (see insets in figure 1).

3.2. Spectral phase modulation of single pulse

An unmodified laser pulse can be described accurately by a Gaussian function. A Gaussian pulse with FWHM duration τ, central frequency ω_0 and pulse intensity E_0 can be written as

$$G(t) = E_0 \exp(-2\ln 2 t^2/\tau^2)\exp(-\imath\omega_0 t) \tag{18}$$

with the frequency representation given by a Fourier transform as

$$G(\omega) = (E_0\tau/2\sqrt{\ln 2})\exp(-\tau^2(\omega-\omega_0)^2/8\ln 2). \tag{19}$$

In what follows, the spectral electric field is written $G(\omega) = |G(\omega)|\,\mathrm{e}^{\imath\psi(\omega)}$, where $|G(\omega)|$ is the amplitude and $\psi(\omega)$ is the phase. In the general case, no analytical Fourier transform exists and the Fourier transform to the time domain is done numerically using a standard FFT [24]. The spectral amplitude is assumed to be a Gaussian as described by equation (19). We first study the effect of a step in the spectral phase in the form

$$\psi(\omega) = \alpha H(\omega - \omega_n), \tag{20}$$

where $H(\omega)$ is the Heaviside step function and α is the magnitude of the step. In the particular case when $\omega_n = \omega_0$, an explicit Fourier transform has been found [6] and the temporal electric field has the following form,

$$G(t) = \frac{E_0}{\sqrt{2\pi}}\cos\frac{\alpha}{2}\exp\left(-\frac{8\ln 2}{9\tau^2}t^2\right)\left(1+\tan\frac{\alpha}{2}\,\mathrm{erfi}\frac{t\sqrt{2\ln 2}}{\tau}\right)\exp(-\imath\omega_0 t), \tag{21}$$

where erfi is the antisymmetric error function [6]. The effect of a single phase step on a Gaussian pulse is demonstrated in figure 2. The step creates a pulse doublet in the time domain, with a π phase jump between the two pulses. The relative height of the two peaks is controlled by the magnitude of the spectral phase step.

In Rydberg systems, the resonances (states) come in series which repeat for every unit of the effective quantum number. It is therefore reasonable to assume that the phase should change in a manner which reflects the periodicity inherent in the system. The effect of a

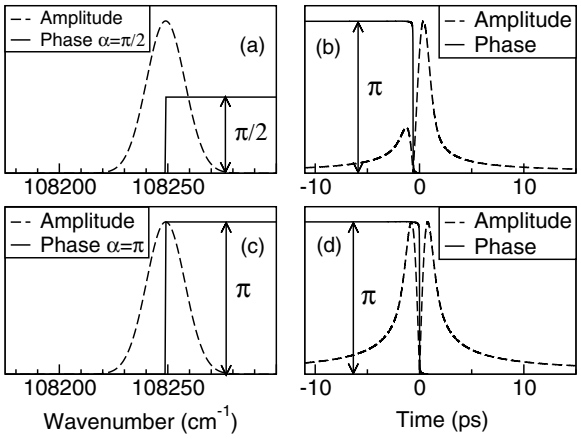

Figure 2. A Gaussian pulse with a single spectral phase step in the frequency (a), (c) and the time domain (b), (d). The magnitude of the spectral phase step is $\alpha = \pi/2$ in (a), (b) and $\alpha = \pi$ in (c), (d).

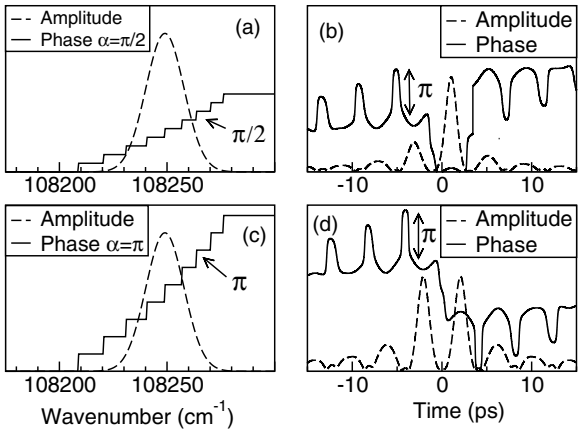

Figure 3. A Gaussian pulse with repeated spectral phase steps in the frequency (a), (c) and the time domain (b), (d). The magnitude of the spectral phase step is $\alpha = \pi/2$ in (a), (b) and $\alpha = \pi$ in (c), (d).

sequence of phase steps (under the same unchanged Gaussian envelope) on the optical pulse is explored in figure 3. The spectral phase $\Psi(\omega)$ can be written as

$$\Psi(\omega) = \alpha \sum_n H(\omega - \omega_n), \tag{22}$$

where $\omega_n \sim (n-\mu)^{-2}$ for a single channel Rydberg series. The behaviour in the time domain is quite analogous to the single phase step case, except that there is now a whole series of peaks approximately separated by the classical period $T_{cl} \sim 4.1$ ps. As before, the relative amplitude of the peaks in the time domain is changed by the magnitude α of the spectral phase steps. Also, in both cases a step of magnitude $\alpha = \pi$ gives peaks symmetric around $t = 0$ in the time domain (see figures 2(d) and 3(d)).

Finally, we examine the effect of a sequence of step-up, step-down phase pulses as shown in figure 4(a) and (c). The corresponding phase function, which aims to reflect the periodicity

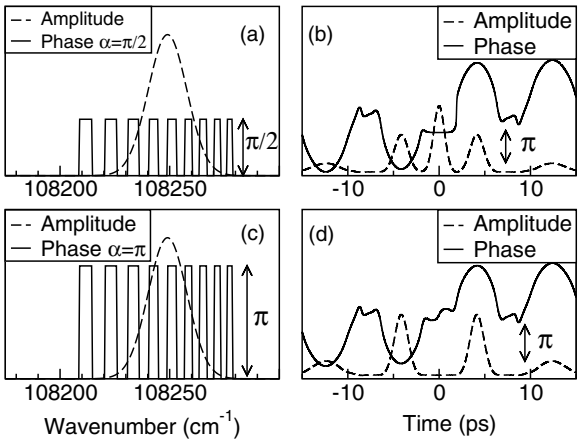

Figure 4. A Gaussian pulse with pulsed spectral phase in the frequency (a), (c) and the time domain (b), (d). The height of the pulses is $\alpha = \pi/2$ in (a), (b) and $\alpha = \pi$ in (c), (d).

of the Rydberg energy levels, can be written as

$$\Psi(\omega) = \alpha \sum_n H(\omega - \omega_n) - H(\omega - \omega_n'), \tag{23}$$

where $\omega_n \neq \omega_n'$ are the positions of the two legs of the pulse. In figure 4 we see that amplitude in the time domain is distributed symmetrically around $t = 0$ irrespective of α, but with the relative height of the central and the flanking peaks determined by the magnitude of α. Here, as in the previous two cases, the temporal phase is relatively insensitive to the magnitude of α in the spectral phase.

4. Results

The branching ratio for autoionizing Xe atoms is calculated by equations (1)–(3) for a single 1 ps Gaussian pulse centred at principal quantum number $\overline{n} = 30.0188$, the position of a $ns_{1/2}$ narrow resonance. Figure 5 shows the branching ratio when scanning the position of one single spectral phase step, as described by equation (20), over one unit of the effective quantum number. It is clear that the position of the phase step has a strong influence on the branching ratio, while the magnitude α of the phase step has a lesser but not insignificant effect, with the $\alpha = \pi$ step having the stronger effect. Overall, the shape of the branching ratio curves changes very little with different magnitudes α of the spectral phase step. Since the amplitude of the phase step influences the relative height of the temporal amplitude, but does not change the temporal phase characteristics much, it is likely that the mechanism depends mostly on the phase. The biggest effect on the branching ratios occurs at the narrow $ns_{1/2}$ resonance, as can be seen from the scaled total photoionization cross-sections included in figure 5.

With only one spectral phase step, control is limited to the resonance located at the centre of the optical pulse. It makes sense to extend the control by repeating the same phase-jump at each resonance under the spectral envelope. We therefore use repeated steps, as described by equation (22) and illustrated in figure 3. The position of the phase steps, which are repeated for every principal quantum number, is scanned as in the previous calculation. Figure 6 shows the resulting branching ratios. We see that, as anticipated, the branching ratios show greater variation, with lower minima and higher maxima. As in the single step case, the position of the

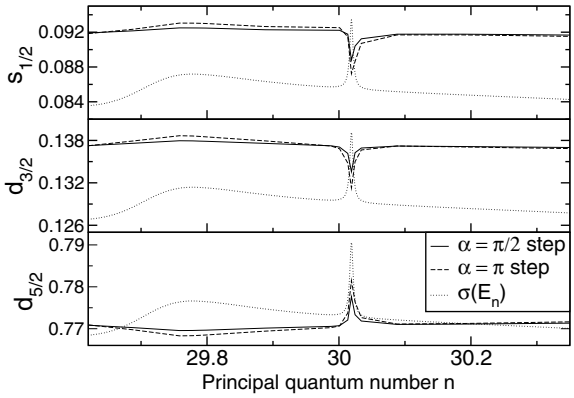

Figure 5. Branching ratio into the three open channels $\epsilon s_{1/2}, \epsilon d_{3/2}$ and $\epsilon d_{5/2}$ as a function of the position of the single spectral phase step (equation (20)) under a constant Gaussian. The magnitude of the step is $\alpha = \pi$ and $\alpha = \pi/2$. A scaled photoionization cross-section is plotted in the background for guidance.

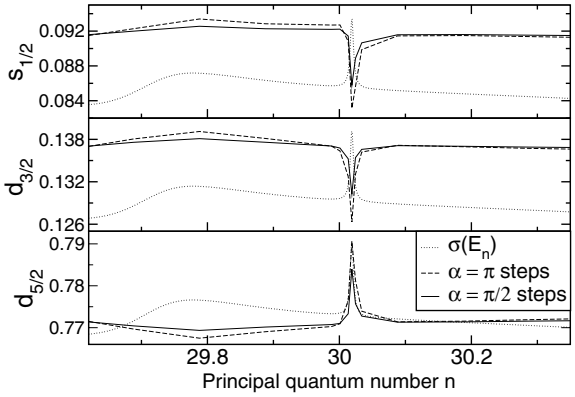

Figure 6. Branching ratio into the three open channels $\epsilon s_{1/2}, \epsilon d_{3/2}$ and $\epsilon d_{5/2}$ as a function of the position of the repeated spectral phase step (equation (22)) under a constant Gaussian. The magnitude of the steps is $\alpha = \pi$ and $\alpha = \pi/2$. A scaled photoionization cross-section is plotted in the background for guidance. The branching ratios show greater variation compared to the calculations with a single spectral phase step.

phase steps is more important than the magnitude α, which again indicates that the temporal phase is more important than the temporal amplitudes. Although the temporal structure of the optical pulse is quite different compared to the single spectral phase step, the shape of the branching curves remains virtually unchanged (compare figures 5 and 6). This indicates that the basic mechanism is the same in both cases and that indeed we simply adapt to the periodicity of the Rydberg system.

Finally, we try to extend the degree of control by using pulsed spectral phases, as described by equation (23) and illustrated in figure 4. The height of the pulses is set to $\alpha = \pi$ and $\alpha = \pi/2$ and one leg of each pulse is fixed at a position which corresponds to a narrow $ns_{1/2}$ resonance. This position is chosen since it gives the greatest change in branching ratio for single and repeated steps (figures 5 and 6). We then scan the other leg of the pulse over one unit of the effective principal quantum number, in complete analogy with the two previous

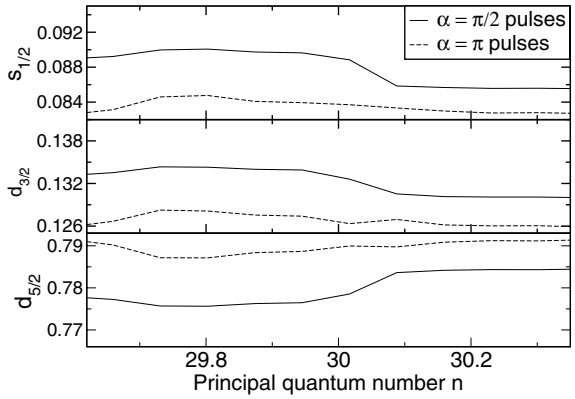

Figure 7. Branching ratio into the three open channels $\epsilon s_{1/2}$, $\epsilon d_{3/2}$ and $\epsilon d_{5/2}$ for a Gaussian pulse with pulsed spectral phase (equation (23)) of height $\alpha = \pi$ and $\alpha = \pi/2$. One leg of the pulse is held fixed at the $ns_{1/2}$ resonance at $\overline{n} \approx 30.019$, and the branching ratio is given as a function of the position of the second leg, which is scanned over one unit of effective principal quantum number. For $n > 30.1$ the branching ratios converge closely on corresponding values of the branching ratios obtained in the previous calculation with repeated steps positioned at the $ns_{1/2}$ resonances.

calculations. The results are shown in figure 7. When the position of the scanned leg is $n > 30.1$, the branching ratios converge very closely on the branching ratios obtained in the previous calculation with repeated steps positioned at the $ns_{1/2}$ resonances, which indicates that the first leg, fixed at the $ns_{1/2}$ resonances, determines the branching ratio, and that the position of the second leg only is important for $n < 30$. For $n < 30.1$ the position of the second leg corresponds broadly to the $nd_{5/2}$ resonances, and leads us to believe that the two phase-jumps act on either resonance in a rather independent manner.

5. Conclusions

The aim of this paper was to explore the potential of the application of novel phase-shaped pulses to Rydberg systems. Our calculations show that there is substantial potential for direct and intuitive control over these systems with shaped pulses. In particular, it is interesting to note that an apparently complicated temporal pulse may have a surprisingly simple structure in the frequency domain. The level of control achieved with simple manipulation of the spectral phase is encouraging, and, as our pulsed-phase calculations indicate, the effects are almost additive in nature, which may simplify intelligent coherent control tremendously (i.e. control based on an understanding of the physics of the system).

Further work has three promising routes. Firstly, one can include the full adjustability of the phase *and* shape the amplitude of the envelope. The parameter space will become intractable by simple mapping methods, and adaptive pulse-shaping and optimization algorithms [34] will be required. Secondly, we aim to elucidate the basic mechanisms of the control process. We are collaborating with Ch Jungen (Orsay, Paris-Sud) to calculate full wavefunctions and probability fluxes so that the dynamics of the system can be inspected more closely. This part of the project also involves a closer study of the complex excitation function, which describes the flow of energy between the electromagnetic field and the quantum system [35]. Finally, we aim to combine pulse shaping techniques with the two pulse schemes discussed in section 3.1 of this paper. Such hybrid schemes should have great potential for efficient control.

Acknowledgments

We thank the Leverhulme Trust for postdoctoral fellowship (AK), and the EPSRC for an Advanced Research Fellowship (HHF). We are also grateful to Ch Jungen (Orsay, Paris-Sud) for useful discussions and encouragement.

References

[1] Brixner T, Pfeifer T, Gerber G, Wollenhaupt M and Baumert T 2004 Optimal control of atomic, molecular and electron dynamics with tailored femtosecond laser pulses *Femtosecond Laser Spectroscopy* ed P Hannaford (New York: Springer) chapter 9
[2] Shapiro M and Brumer P 2003 Coherent control of molecular dynamics *Rep. Prog. Phys.* **66** 859
[3] Weinacht T C, Ahn J and Bucksbaum P H 1999 Controlling the shape of a quantum wavefunction *Nature* **397** 233
[4] Fielding H H 2005 Rydberg wavepackets in molecules: from observation to control *Annu. Rev. Phys. Chem.* **56** 91
[5] Weiner A M 2000 Femtosecond pulse shaping using spatial light modulators *Rev. Sci. Instrum.* **71** 1929
[6] Renard M, Chaux R, Lavorel B and Faucher O 2004 Pulse trains produced by phase-modulation of ultrashort optical pulses: tailoring and characterization *Opt. Express* **12** 473
[7] Heller E J 1981 Frozen Gaussians: a very simple semiclassical approximation *J. Chem. Phys.* **75** 2923
[8] Shalashilin D V and Child M S 2004 The phase space CCS approach to quantum and semiclassical molecular dynamics for high-dimensional systems *Chem. Phys.* **304** 103
[9] Henle W A, Ritsch H and Zoller P 1987 Rydberg wave packets in many electron atoms excited by short laser pulses *Phys. Rev.* A **36** 683
[10] Fielding H H 1994 Rydberg electron wavepacket dynamics in molecular hydrogen *J. Phys. B: At. Mol. Opt. Phys.* **27** 5883
[11] Robicheaux F and Hill W T III 1996 Autoionizing Rydberg wave packets *Phys. Rev.* A **54** 3276
[12] Ramswell J A and Fielding H H 1998 Angle-resolved spin-orbit autoionisation dynamics of Rydberg electron wave packets in Ar: a time-dependent MQDT approach *J. Chem. Phys.* **108** 7653
[13] Texier F and Jungen Ch 1998 Nuclear-electronic wave-packet dynamics in perturbed Rydberg states of molecular hydrogen *Phys. Rev. Lett.* **81** 4329
[14] Millet M, Aymar M, Luc-Koenig E and Lecomte J-M 2002 Dynamics of autoionizing wavepackets in Calcium *J. Phys. B: At. Mol. Opt. Phys.* **35** 875
[15] Aymar M, Greene C H and Luc-Koenig E 1996 Multichannel Rydberg spectroscopy of complex atoms *Rev. Mod. Phys.* **68** 1015
[16] Greene C H and Jungen Ch 1985 Molecular applications of quantum defect theory *Adv. At. Mol. Phys.* **21** 51
[17] Lu K T 1971 Spectroscopy and collision theory. The Xe absorption spectrum *Phys. Rev.* A **4** 579
[18] Johnson W R, Cheng K T, Huang K-N and Le Dourneuf M 1980 Analysis of Beutler-Fano autoionizing resonances in the rare-gas atoms using the relativistic multichannel quantum-defect theory *Phys. Rev.* A **22** 989
[19] Wörner H J, Grütter M, Vliegen E and Merkt F 2005 Role of nuclear spin in photo-ionization: hyperfine-resolved photoionization of Xe and multichannel quantum defect theory analysis *Phys. Rev.* A **71** 052504
[20] Verlet J R R, Stavros V G, Minns R S and Fielding H H 2002 Controlling the angular momentum composition of a Rydberg electron wave packet *Phys. Rev. Lett.* **89** 263004
[21] Verlet J R R, Stavros V G, Minns R S and Fielding H H 2003 Controlling the radial dynamics of Rydberg wavepackets in Xe using phase-locked optical pulse sequences *J. Phys. B: At. Mol. Opt. Phys.* **36** 3683
[22] Martin W C and Wiese W L 1996 Atomic spectroscopy *Atomic, Molecular and Optical Physics Handbook* ed G W F Drake (Woodbury, NY: AIP) chapter 10, p 135 http://physics.nist.gov
[23] Arfken G B and Weber H J 1995 *Mathematical Methods for Physicists* 1st edn (New York: Academic)
[24] Press W, Vetterling W, Teukolsky S and Flannery B 1992 *Numerical Recipes in Fortran* 2nd edn (Cambridge: Cambridge University Press)
[25] Cundiff S T and Jun Y 2003 Colloqium: femtosecond optical frequency combs *Rev. Mod. Phys.* **75** 325
[26] Jones R R, Schumacher D W, Gallagher T F and Bucksbaum P H 1995 Bound-state interferometry using incoherent light *J. Phys. B: At. Mol. Opt. Phys.* **28** L405
[27] Noel M W and Stroud C R Jr 1996 Excitation of an atomic electron to a coherent superposition of macroscopically distinct states *Phys. Rev. Lett.* **77** 1913

[28] Averbukh I Sh and Perelman N F 1989 Fractional revivals: universality in the long-term evolution of quantum wave packets beyond the correspondence principle dynamics *Phys. Lett.* A **139** 449
[29] Carley R E, Boleat E D, Minns R S, Patel R and Fielding H H 2005 Interfering Rydberg wave packets in Na *J. Phys. B: At. Mol. Opt. Phys.* **38** 1907
[30] Van Woerkom L D and Cooke W E 1986 Complementary branching ratios by satellite excitation *Phys. Rev. Lett.* **57** 1711
[31] van Leeuwen R, Bajema M L and Jones R R 1999 Coherent control of the energy and angular distribution of autoionized electrons *Phys. Rev. Lett.* **82** 2852
[32] Connerade J P 1983 On Rydberg series of autoionising resonances *J. Phys. B: At. Mol. Phys.* **16** L329
[33] Connerade J P 1985 Autoionising line shapes *J. Phys. B: At. Mol. Phys.* **18** L367
[34] Judson R S and Rabitz H 1992 Teaching lasers to control molecules *Phys. Rev. Lett.* **68** 1500
[35] Shapiro M 1990 Fundamental theory of photodissociation with pulses *Half Collision Resonance Phenomena in Molecules, AIP Conference Proceedings 225* ed M Garcia-Sucre, G Raseev and S Ross (New York: AIP) p 230